TIME DOMAIN IDENTIFICATION OF A HELICOPTER USING MINIMAL REPRESENTATION AND TIME DELAYS

Ongun Hazar Aslandoğan
Research Associate
Technical University of Munich

Gönenç Gürsoy
Senior Flight Dynamicist
Simulator Division
Volocopter GmbH

İlkay Yavrucuk
Professor and Head of Institute
Technical University of Munich

ABSTRACT

This paper presents a standalone time domain approach to identify the dynamics of a full-scale helicopter in both hover and forward flight. A high-fidelity nonlinear helicopter model of a commercial 3t classd helicopter is employed to generate the dataset, which consists of 3211 and 2311 type inputs for identification and frequency sweep type maneuvers for verification. The output error algorithm is used in conjunction with the Levenberg Marquardt routine in time domain to estimate the parameters of the state space model structure. A systematic model reduction routine is employed to eliminate redundant parameters from the model structure, thereby achieving a minimal representation of the dynamics. To account for the higher-order dynamics induced by the rotor, time delays are introduced into the state and control matrices in the relevant derivatives. The identified models are verified in frequency domain by demonstrating that the errors fall within the acceptable bounds. Furthermore, the obtained set of parameters is shown to be consistent with the values reported in the literature.

NOTATION

*

Symbols

A, B, C, D state space representation matrices

a_x, a_y, a_z specific accelerations in body fixed frame, $\mathrm{ft/s^2}$

$\mathrm{CR_i}$ Cramer-Rao bound of the ith parameter

$\overline{\mathrm{CR_i}}$ normalized Cramer-Rao bound of the ith parameter

f frequency, $\mathrm{rad/s}$

$\mathcal{F}$ Hessian matrix

$\mathcal{G}$ gradient vector

$H(f)$ frequency response function

I identity matrix

I_i insensitivity of the ith parameter

$\overline{I_i}$ normalized sensitivity of the ith parameter

J maximum likelihood cost function

N number of samples

p, q, r angular rates in body fixed frame, $\mathrm{deg/s}$

R measurement noise covariance matrix

t time, s

$\boldsymbol{u}$ control input vector

u, v, w translational velocities in body fixed frame, $\mathrm{ft/s}$

$\boldsymbol{x}$ state vector

$\boldsymbol{y}$ output vector

$\boldsymbol{z}$ measurement vector

δ_{coll} collective control, $\%$

δ_{lat} lateral cyclic control, $\%$

δ_{long} longitudinal cyclic control, $\%$

δ_{ped} pedal control, $\%$

ε frequency domain error function

θ, ϕ, ψ pitch, roll and yaw angles, deg

$\mathbf{\Theta}$ unknown parameter vector

λ Levenberg-Marquardt parameter

σ standard deviation

τ time delay, s

*

Acronyms

AEE Allowable Error Envelopes

CR Cramer-Rao

DFT Discrete Fourier Transformation

DoF Degree of Freedom

EASA European Union Aviation Safety Agency

LM Levenberg Marquardt

MIMO Multi Input Multi Output

MUAD Maximum Unnoticeable Added Dynamics

RMSE Root Mean Square Error

INTRODUCTION

Mathematical models of dynamics systems aim to represent real-life processes by employing physical laws and principles. Such models of flight vehicles relate the control inputs provided to the system to its dynamic response with a certain degree of accuracy. Modeling the dynamic behavior of an aircraft in flight poses significant challenges, particularly in the case of rotorcraft, due to the intricate nature of the underlying physics. One approach to obtaining mathematical models representing the dynamics between input and output signals is through system identification. The discipline of system identification focuses on the determination of the mathematical model that produces the best-fitting responses when the same inputs are provided to the model. The mathematical models acquired can be utilized to analyze the stability characteristics, create flight stability augmentation systems, validate aerodynamic experimental findings, and create and improve flight simulation models.

In system identification, the choice of identification procedure is influenced by the characteristics of the system being examined. Linear models are often preferred due to their simplicity and ease of use, but the choice between frequency domain and time domain methods depends on the objectives of the analysis and the available data. Frequency domain methods focus on transfer function identification, offering direct insights into system stability and better measurement noise handling. They also avoid divergence during iterations, simulation of the model response is not required. This makes frequency domain methods particularly well-suited for lengthy maneuvers, such as frequency sweeps. On the other hand, time domain methods are often more intuitive and avoid errors associated with transforming data from the time domain to the frequency domain. Additionally, the result is an estimated state-space system. These methods employ shorter 3211, 2311 or doublet type multistep maneuvers as the system response is simulated during iterations.

The complexity and the structure of the mathematical model also depend on the dynamics of the system. Transfer functions, which uniquely define the relationship between input-output pairs, become cumbersome when dealing with MIMO systems where responses are coupled across multiple inputs and outputs. In such cases, state-space models are more appropriate. For instance, a fixed-wing aircraft can typically be modeled as a rigid body and exhibits uncoupled longitudinal and lateral dynamics due to planar symmetry. In contrast, helicopters exhibit inherent coupling between longitudinal and lateral responses due to the rotor dynamics. This coupling, which varies significantly with operating conditions, makes the state-space model structure more suitable compared to transfer functions to accurately represent the MIMO characteristics of helicopter dynamics.

Even though state space systems are better suited for MIMO systems, time domain identification of full-scale helicopter dynamics presents significant challenges. Helicopters, particularly in hover, exhibit inherently unstable dynamics that can lead to intermediate divergence during simulations. Furthermore, the data collected during flight is susceptible to measurement noise. Accurate estimation of aerodynamic derivatives is required in aircraft system identification, which is only possible with a physical model structure. Nevertheless, due to the non-unique nature of the state space systems, there can be infinitely many state-space representations for the same set of inputs and outputs, which may result in multiple solutions during estimation.

Moreover, a full-scale helicopter exhibits higher-order dynamics, primarily due to the presence of the rotor. The coupled pitch to roll responses, along with input delays caused by the indirect control of the tip path plane through blade pitch angles, prevents the helicopter from being accurately represented by a simple six-degree-of-freedom model.

The majority of the existing research on full-scale helicopter system identification has favored frequency domain methods. Early examples of rotorcraft system identification include matching frequency responses of S-55 and Bo-105 helicopters (Refs. 1, 2). Afterward, Tischler et al. identified transfer function models for the XV-15 tiltrotor and the Bell214-ST using frequency responses and frequency sweep maneuvers (Refs. 3,4). Seher-Weiss et al. carried out the identification of the H135 helicopter in the frequency domain, incorporating additional rotor and engine dynamics (Refs. 5–7). A recent overview of the frequency domain system identification research is published by Berger and Tobias et al. Applications of time domain system identification methods to small-scale unmanned helicopters have been studied by Li et al. (Ref. 8), Shim et al. (Ref. 9), Khaligh et al. (Ref. 10), and Grauer et al. (Ref. 11). (Ref. 12), however, applications to full-scale helicopters are limited.

This study alleviates the shortcomings of the time domain system identification and remedy the challenges in rotorcraft system identification with a systematic approach. In this work, the identification of full-scale helicopter dynamics in time domain by utilizing a standalone output error based identification framework is carried out. For parameter estimations, the well recognized maximum likelihood output error method (Ref. 13) is utilized. A physics-based core helicopter model that resembles a 3T class helicopter is used as the truth model to generate the data set (Ref. 14). For time domain identification, 3211 and 2311 type maneuvers are conducted in two flight conditions, hover and 70kts forward flight. To overcome the intermediate divergence during time domain simulations, the output error method is coupled with the Levenberg-Marquardt algorithm (Refs. 13,15), which prevents divergence between iterations and redirects the solution towards the steepest descend in the cost function. A minimal representation of the model structure is achieved by using a Hessian-based systematic model reduction approach (Ref. 16), where the redundant parameters in the state space model structure are eliminated from the model depending on their Cramer-Rao bounds and insensitivities. With this approach, the confidence in the parameter estimates is improved. The higher-order dynamics arising from the presence of the rotor are accommodated by the inclusion of state and control delays in related derivatives, which are then identified with the rest of the parameters. Finally, the identified system is verified in the frequency domain using frequency sweep maneuvers.

METHODOLOGY

Mathematical Model

In flight vehicle system identification, the determination of the mathematical model structure depends on the specific application. The mathematical model structure must be physics-based, as the accurate estimation of the aerodynamic derivatives is of paramount importance. Since the identification is carried out in the time domain, a state space representation for the helicopter dynamics is employed. The set of equations of motion linearized at a trim condition is expressed as:

$$\dot{\boldsymbol{x}} = A\boldsymbol{x} + B\boldsymbol{u} \tag{1}$$

$$\boldsymbol{y} = C\boldsymbol{x} + D\boldsymbol{u} \tag{2}$$

Where $\boldsymbol{x} = [u\, w\, q\, \theta\, v\, p\, \phi\, r]^T$ is the state vector, consisting of the linear velocities, angular rates and Euler angles, $\boldsymbol{u} = [\delta_{long}\, \delta_{lat}\, \delta_{coll}\, \delta_{ped}]^T$ is the control vector of cyclic, collective and pedal controls, and $\boldsymbol{y} = [a_x\, a_z\, q\, \theta\, a_y\, p\, \phi\, r]^T$ is the measurement vector consisting of accelerometer and gyroscope measurements. A, B, C and D are system, control, output and feed-through matrices, respectively.

The aforementioned dynamics include blade lapping, lead-lag, coning/inflow, and yaw/engine dynamics. In order to reflect these transient changes in flow characteristics, delay arrays have been proposed by Jategaonkar (Ref. 13). It is essential that the delays introduced into the model structure are positioned appropriately. Upon examination, it is determined that the higher-order dynamics resulting from input delay and pitch-to-roll coupling are the most pronounced. The input delay is a result of the indirect control of the tilting of the tip path plane through the use of cyclic controls. In order to initiate flapping, the pitch angles of the blades are modified with the use of cyclic controls, resulting in a phase shift in the flapping. The coupling between pitch and roll is a consequence of the gyroscopic effect of the rotor. When the rotor has a non-zero angular rate in the body x-y plane, a moment is generated in the perpendicular axis, resulting in a non-zero angular rate. Consequently, time delays are introduced in the cyclic control derivatives of the pitch and roll moments to account for the input delay, and the p and q derivatives of the pitch and roll moments to reflect the pitch-roll coupling due to the gyroscopic effect. The implementation of delays can be observed in equations 3 and 4.

$$\begin{aligned}\dot{p} = L_p p(t-\tau_1) + \ldots + L_q q(t-\tau_2) + \ldots \\ + L_{\delta_{long}} \delta_{long}(t-\tau_3) + \ldots + L_{\delta_{lat}} \delta_{lat}(t-\tau_4)\end{aligned} \tag{3}$$

$$\begin{aligned}\dot{q} = M_p p(t-\tau_5) + \ldots + M_q q(t-\tau_6) + \ldots \\ + M_{\delta_{long}} \delta_{long}(t-\tau_7) + \ldots + M_{\delta_{lat}} \delta_{lat}(t-\tau_8)\end{aligned} \tag{4}$$

The parameter set designated as τ, represents the time delays in these equations. The value of each time delay is unknown. Hence, the set of time delays is implemented as parameters to be identified with the restriction that they cannot obtain negative values.

Maximum Likelihood Output Error Method

Based on the maximum likelihood estimation theory, the output error method is a powerful estimation algorithm which can be used for linear or nonlinear systems with any level of intricacy. It is an iterative method that requires the estimation of system responses to be simulated multiple times at each iteration until a local minimum is reached. Following the derivations in (Ref. 13), for vector of observations $\boldsymbol{z}$ and vector of model outputs $\boldsymbol{y}$, the cost function reduces to the form as shown in eq.

5 and the measurement noise covariance matrix R is calculated from eq. 6.

$$J(\mathbf{\Theta}) = \det(R) \tag{5}$$

$$R = \frac{1}{N}\sum_{k=1}^{N}\left[\boldsymbol{z}(t_k) - \boldsymbol{y}(t_k)\right]\left[\boldsymbol{z}(t_k) - \boldsymbol{y}(t_k)\right]^T \tag{6}$$

Here, $\mathbf{\Theta}$ is the vector of identification parameters, which are in this case the derivatives and time delays in the state and control matrices. From the Gauss-Newton Algorithm, the parameter update vector $\Delta\mathbf{\Theta}$ is then calculated using the Hessian matrix $\mathcal{F}$ and gradient vector $\mathcal{G}$ from eqs. 7, 8, 9.

$$\Delta\mathbf{\Theta} = \mathcal{F}^{-1} - \mathcal{G} \tag{7}$$

$$\mathcal{F} = \sum_{k=1}^{N}\left[\frac{\partial \boldsymbol{y}(t_k)}{\partial \mathbf{\Theta}}\right]^T R^{-1}\left[\frac{\partial \boldsymbol{y}(t_k)}{\partial \mathbf{\Theta}}\right] \tag{8}$$

$$\mathcal{G} = -\sum_{k=1}^{N}\left[\frac{\partial \boldsymbol{y}(t_k)}{\partial \mathbf{\Theta}}\right]^T R^{-1}[\boldsymbol{z}(t_k) - \boldsymbol{y}(t_k)] \tag{9}$$

Finally, the parameter update at iteration step i is performed with eq. 10 and iteration is continued until convergence is achieved.

$$\mathbf{\Theta}_{i+1} = \mathbf{\Theta}_i + \Delta\mathbf{\Theta} \tag{10}$$

The Gauss-Newton algorithm is an effective method for identifying the dynamics of a system when the initial values of the identification parameters are not significantly different from the values at the local minimum cost, or when the system is linear. However, when identifying the dynamics of a full-scale helicopter using simulations that exceed a few seconds in length, the algorithm is susceptible to divergence.

To remedy this common problem of intermediate divergence in time domain output error method, Levenberg-Marquardt (LM) parameter update algorithm (Ref. 15) is incorporated into the Gauss-Newton algorithm. It introduces the LM parameter λ to the parameter update calculation, as shown in eq. 11, and it follows a logic structure such that the increase in cost function between iterations is prevented.

$$(\mathcal{F} + \lambda I)\Delta\mathbf{\Theta} = -\mathcal{G} \tag{11}$$

The algorithm requires an initial estimation of the LM parameter, which is then adjusted to achieve the direction of maximum cost function reduction within the inner LM loop. The incorporation of the inner loop calls the simulation of the system response two additional times at each iteration, thereby increasing the computational overhead.

Model Reduction

A MIMO model is the ideal representation of full-scale helicopter dynamics in the time domain, as a state space system is particularly suited to such applications. However, it should be noted that state space systems are not unique by definition. Consequently, there are an infinite number of state space systems that produce the same model output for the same input data. It is possible that identification with the fully populated system and control matrices may result in the estimation of non-physical parameters, even when convergence is achieved. Given the paramount importance of accurately estimating aerodynamic derivatives in the identification of flight vehicle systems, it is essential to have a minimal representation of the system with high confidence in the parameter estimates. A solution to this problem is presented by Gursoy et al. (Ref. 17), where the adaptive learning algorithm is implemented to determine a unique and optimal model structure based on bias variance tradeoff.

This work focuses on rotorcraft system identification with a standalone framework based on the output error algorithm. Accordingly, a systematic approach is carried out to eliminate redundant parameters from the model structure and increase confidence in the remaining parameters in accordance with the methodology outlined in (Ref. 16). This approach employs the Hessian matrix to calculate the Cramer-Rao (CR) bounds and insensitivities I of each identification parameter. These parameters are used as mathematical metrics to assess the redundancy of the model parameters. Conveniently, the Hessian matrix is readily available from eq. 8 of the output error algorithm, eliminating the need for partial derivative calculation for model reduction purposes. The Cramer-Rao bounds define the minimum standard deviation for an identification parameter i as:

$$\sigma_i \geq \mathrm{CR}_i \tag{12}$$

$$\mathrm{CR}_i = \sqrt{(\mathcal{F}^{-1})_{ii}} \tag{13}$$

These bounds are calculated using equation 13, where the Hessian matrix represents the curvature of the cost function with respect to the parameter estimate Θ_i. Consequently, Cramer-Rao bounds reflect the change in the cost function to the variation in that model parameter. In order to obtain a meaningful comparison, CR values are normalized with respect to the parameter value.

$$\overline{\mathrm{CR}_i} = \left|\frac{\mathrm{CR}_i}{\Theta_i}\right| \times 100\%. \tag{14}$$

Insensitivities is the other basis to assess the importance of model parameters. It represents the insensitivity of the cost function to the changes in Θ_i, as calculated from eq. 15.

$$I_i = \frac{1}{\sqrt{\mathcal{F}_{ii}}} \tag{15}$$

Similarly, the values are normalized to make them comparable.

$$\bar{I}_i = \left| \frac{I_i}{\Theta_i} \right| \times 100\% \tag{16}$$

The CR bounds and insensitivities are geometrically related, where the CR bounds define the upper limit for insensitivities (Ref. 18).

$$\bar{I}_i \leq \overline{\mathrm{CR}}_i \tag{17}$$

The procedure is initiated with the model fully populated with the identification parameters (Ref. 16). In the absence of prior information on the values of the model parameters, the initial conditions of the parameters are set to zero, as is the case in this paper. Once the convergence is achieved, the normalized insensitivities are calculated and the parameter with the largest insensitivity is removed from the model structure by setting it to zero. The remaining parameters are then reset to their initial values and the parameter estimation process is restarted. This process is repeated until all remaining parameters have insensitivity values below 10%. Next, CR bounds are examined, as large CR values indicate correlation between parameters. The model reduction is continued by the removal of the parameters with the largest CR value at each convergence. The reduction procedure is terminated when all parameters obey the guideline of $\overline{\mathrm{CR}}_i \leq 20\%$. During this procedure, the root mean square error (RMSE), obtained from eq. 18 must be monitored after each parameter drop. If removal of a parameter results in a significant increase in the RMSE, the procedure is terminated.

$$\mathrm{RMSE} = \sqrt{\left(\frac{1}{N \cdot n_o}\right) \sum_{i=1}^{N} \left[(\boldsymbol{z}-\boldsymbol{y})^T (\boldsymbol{z}-\boldsymbol{y}) \right]} \tag{18}$$

The adequate model structure can be obtained by plotting the variation of the RMSE with the number of parameters dropped and selecting the model with the lowest cost value. For helicopters, the guideline for appropriate time domain model fit is given to be $\mathrm{RMSE} \leq 1.0$ to 2.0 (Ref. 16). By dropping insensitive and correlated parameters from the identification model, a minimal representation of the model structure is achieved, that is, the model structure with the smallest set of parameters that is sufficient to reflect the important system characteristics. With this representation, the accuracy of the remaining parameter estimates is increased, meaning that they converge closer to their actual values. Although this approach provides a systematic manner to achieve a minimal model representation, the uniqueness of the final model structure is not guaranteed.

IMPLEMENTATION AND RESULTS

In this work, the dynamics of a full-scale helicopter are identified in time domain for two flight conditions using a standalone time domain identification framework.

Table 1. List of maneuvers at each trim condition

	Hover	70 knots
3211 in 2 directions in all controls	8	8
2311 in 2 directions in all controls	8	8
Frequency Sweep in all controls	4	4

The flight conditions are selected to be hover and forward flight with 70 knots, as the helicopter shows distinct characteristics in these conditions. The truth model is trimmed to the desired trim condition and the specified inputs for identification and for verification are executed starting from trim. In the course of maneuvers, low frequency controllers are employed to prevent the deviation of the aircraft far from the trim condition. The gyroscope and accelerometer measurements are recorded, and the data is corrupted with white measurement noise to mimic real-life test scenarios. Table 1 shows the list of maneuvers in the data set for each trim condition. In order to carry out identification in time domain, a total of 16 distinct maneuvers are employed in each flight condition. These comprise 3211 and 2311 multistep inputs in the longitudinal cyclic, lateral cyclic, collective and pedal channels, and are applied in both directions. The frequency sweep maneuvers are used to verify the identified model in all excitation channels under two operating conditions. The identification is carried out by estimating the coupled 6DoF model structure with all 16 maneuvers simultaneously. The initial step is to reduce the state space model structure without time delays in order to obtain a minimal representation. As no prior information regarding the parameter values is considered, the parameter estimates are initiated with zero. The appropriate model structure is then selected from the RMSE variation plot and the identification is initiated once more with time delays introduced to the model structure. The time domain identification results are presented for all excitation channels, but only the states with higher importance for each excitation are presented for brevity.

Finally, the identified mathematical models are verified in the frequency domain using the frequency sweep maneuvers. The objective is to evaluate the discrepancy between the truth model and the identification model responses in terms of magnitude and phase characteristics. For this purpose, the frequency response functions H of the time domain input-output pairs are calculated. Given that the collected data has a discrete sampling, discrete Fourier transformation (DFT) is employed. In order to reduce the side lobe leakage in the frequency domain transformations, multiple Hanning windows are utilized. The errors between the frequency response functions are calculated using the formula given in 19.

$$\varepsilon(f) \equiv \frac{H_{sim}(f)}{H_{flight}(f)} \tag{19}$$

The obtained errors are compared with the maximum unnoticeable added dynamics (MUAD) (Ref. 19) bounds and allowable error envelopes (AEE) (Ref. 20). The boundaries of MUAD are constructed with pilot testing, such that the errors within these bounds cannot be noticed by a pilot. In the vicinity of $1 rad/s$ and $10 rad/s$, the bounds get narrower, which corresponds to the operational regime of the pilot and is the most crucial frequency bandwidth for identifying flight systems. The bounds of MUAD are employed in the literature to validate identified models (Refs. 17, 21–23). While the MUAD bounds are constructed by handling quality assessment, AEE are constructed by pilot opinion on task performance. An identified model with errors within these bounds is considered to be satisfactory. For conciseness, only the cyclic tests are presented in this section, as they clearly demonstrate the impact of the included time delays in the system. The 2311 type maneuvers in the collective and pedal channels can be found in Appendix A.

Identification in Hover

The first examined case is identification of dynamics in hover. As previously outlined, the initial step is to reduce the 6DoF state space model to obtain a minimal representation of the system. The coupled linearized equations of motion is constructed by substituting known elements in the system matrix, leaving the remaining parameters in the system and control matrices as identification parameters. The fully populated model structure is converged to a local minimum solution, and the parameters that do not satisfy the insensitivity and Cramer-Rao criteria are removed from the model one by one. For illustrative purposes, this procedure is carried out until all parameters are removed from the model and the RMSE error variation is plotted as shown in fig. 1. Until a certain number of parameters are dropped, the oscillations in the cost function indicate that the remaining parameters are in fact sufficient to represent the overall characteristics of the system. If too many parameters are removed, the system response cannot be represented by the remaining set of parameters and the RMSE increases. From this analysis, the appropriate model is selected as the one with the lowest RMSE, which is the model with 29 parameters removed. In addition, the selected model obeys the guideline of $\mathrm{RMSE} \leq 1.0$ to 2.0 for the time domain fit. At this stage, it is important to monitor the system response of the selected model structure. This is especially important for the identification of helicopter dynamics, as the dynamics of higher order dynamics due to the rotor must be represented by the selected model. Two different model structures with similar cost values may have different characteristics in the high frequency behavior because the effect of such higher frequency oscillations is minimal in the RMSE error.

In hover condition, parameters X_v, X_w, X_r, X_{lat}, X_{coll}, Y_p, Y_q, Y_u, Y_w, Y_{long}, Y_{lat}, Y_{coll}, Y_{ped}, Z_u, Z_v Z_p, Z_q, Z_{long}, Z_{lat},

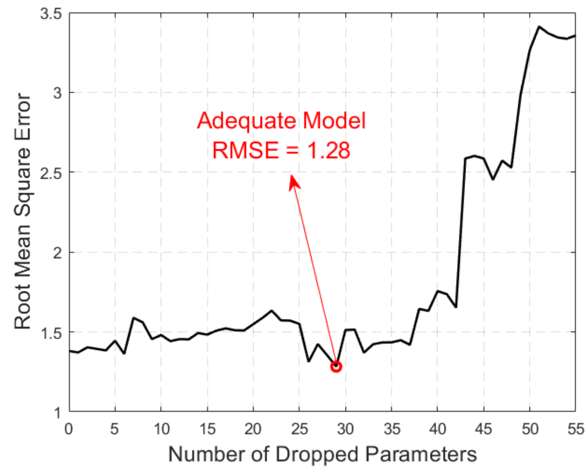

Figure 1. Variation of RMSE through model reduction in hover

Z_{ped}, L_w, L_{coll}, L_{ped}, M_v, M_w, M_{coll}, M_{ped}, N_u and N_{long} are dropped from the model. The obtained model is evaluated in both time and frequency domains to assess its adequacy. The analysis showed that the identified model show satisfactory results in maneuvers with the collective and pedal channels in both time and frequency domains. When the cyclic tests are compared, it is observed that the on-axis angular rate response of the cyclic tests show good agreement with the truth model, while the off-axis responses cannot represent the truth model dynamics at higher frequencies. To account for the higher order dynamics from the rotor, the time delays are introduced into the model structure as described in the Methodology section, and the identification is run for the final time to estimate the time delays and refine the solution. This two-step approach to identify time delays prevent unreasonable estimates for the time delays in the presence of redundant parameters and avoid accidental removal of time delays from the model structure.

The objective is to enhance the confidence of parameter estimates and obtain aerodynamic derivative values close to their physical values with a minimal representation of the system. The static stability of a helicopter for a variation of angle of attack is assessed using the M_w derivative. In hover, the lift increase on both the retreating and advancing rotor blades is similar, making the helicopter neutrally stable with a M_w value near zero. Consequently, M_w is removed from the model structure in hover due to high insensitivity. The dihedral effect is indicated by the L_v derivative. The helicopters have a stabilizing tendency to roll back to level flight when a sideslip occurs, therefore the sign of L_v is negative. Helicopters also exhibit directional stability, with a positive N_v due to the tail rotor in hover. The heave stability, represented by the Z_w derivative, is negative, as an increase in vertical velocity leads to higher rotor thrust. In this work, the values and signs of the important aerody-

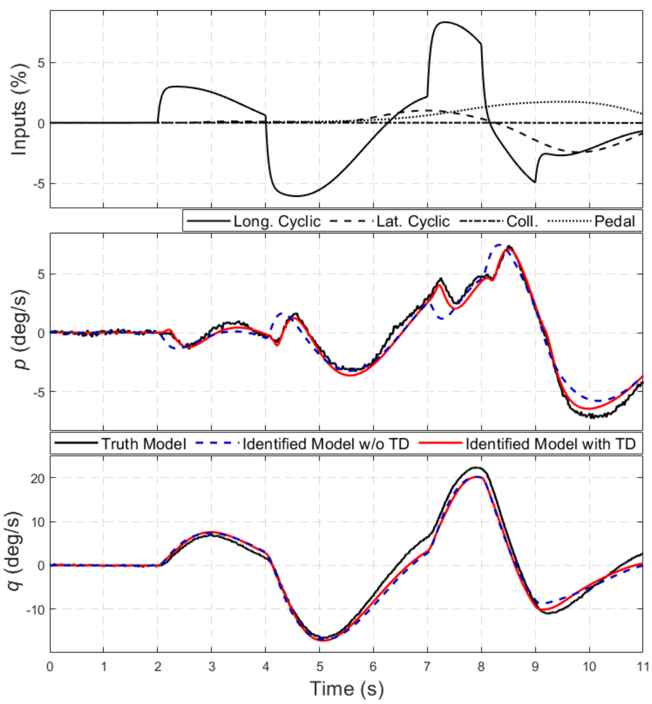

Figure 2. Time domain identification results - longitudinal cyclic 2311 input in positive direction during hover

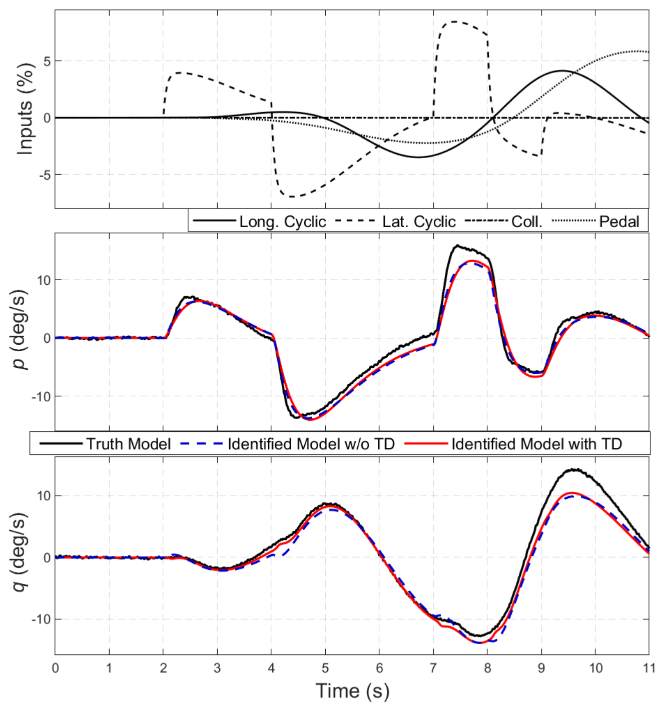

Figure 3. Time domain identification results - lateral cyclic 2311 input in positive direction during hover

namics derivatives, which also include M_u, X_u, X_v, Y_u and Y_v, are in accordance with the presented values for similar helicopters as outlined by Padfield (Ref. 24). Both the dropped and identified parameters, along with their converged values, CR bound and insensitivities can be found in Appendix B.

The longitudinal and lateral cyclic responses of the identified model with and without time delays and the nonlinear truth model are shown in figs. 2 and 3. The impact of the time delays in the time domain response is best observed in the off-axis response of the longitudinal cyclic tests, as shown in fig 2. The roll rate response of the truth model lags behind the identified model without time delays. The oscillation of the roll rate due to the pitch rate is a result of the gyroscopic effect of the rotor. A 6DoF state space model structure is not sufficient to represent this transient effect. With the utilization of time delays in pitch and roll derivatives, such dynamics can be represented with the identified model. The verification of the cyclic results in frequency domain is presented in figs. 4 5, where the frequency sweep responses from the truth model and the identified model are transformed into frequency domain via discrete Fourier transform with windowing. The magnitude and phase errors between the two signals are plotted along with the MUAD bounds and AEE. These bounds construct the allowable error limits for the identified model fit to be considered satisfactory. The error plots indicate a good model fit for the magnitude characteristics of all signal pairs and phase characteristics of the on-axis angular rates. The phase error of the roll rate, as shown in fig. 9, clearly illustrates the inability of the no time delay model to capture the lag of the truth model, which was initially observed in Fig. 2. The employment of time delays bring the error within the acceptable bounds in the frequencies where the coherence function is greater than 0.8. A similar improvement can be seen in fig. 5, where the off-axis pitch response shows unacceptable error characteristics in high frequencies in the absence of time delays. However, this enhancement with time delays is less pronounced in time domain plots than in the longitudinal cyclic tests. This analysis demonstrates that the data set used for time domain identification in this paper is sufficient to reflect the subtle higher-order dynamics in the off-axis responses. Furthermore, this analysis demonstrates the importance of monitoring model responses in both time and frequency domains, as some dynamics can be difficult to detect in one of the domains.

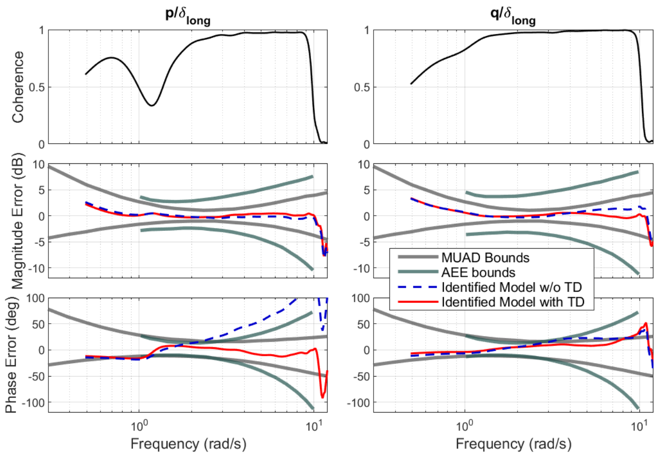

Figure 4. q/δ_{long} **and** p/δ_{long} **pairs with error bounds - longitudinal cyclic frequency sweep maneuver in hover**

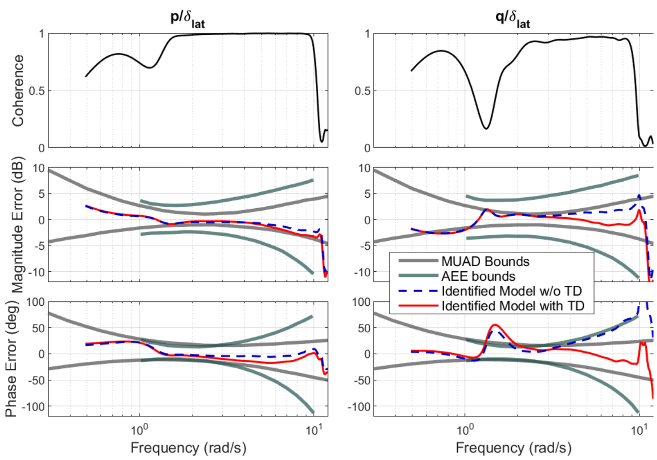

Figure 5. q/δ_{lat} **and** p/δ_{lat} **pairs with error bounds - lateral cyclic frequency sweep maneuver in hover**

Identification in Forward Flight

Forward flight at 70 knots of speed is the second trim condition examined. The procedure followed is similar to the one for hover, where a total of 16 generated test data consisting of 3211 and 2311 type maneuvers are used for identification, as shown in table 1. Starting from zero initial conditions, the model reduction routine is carried out until all parameters are removed from the model structure. Figure 6 shows the RMSE with respect to the number of parameters dropped. When around 20 parameters are removed from the model, the cost function exhibits a clear decrease compared to the fully populated structure. As the model structure is overpopulated when all parameters are present, the output algorithm cannot find a lower cost value, and the iteration is stuck at a local minimum. The removal of redundant parameters leads to a better representation of the dynamics of the system. On the other hand, the removal of crucial parameters

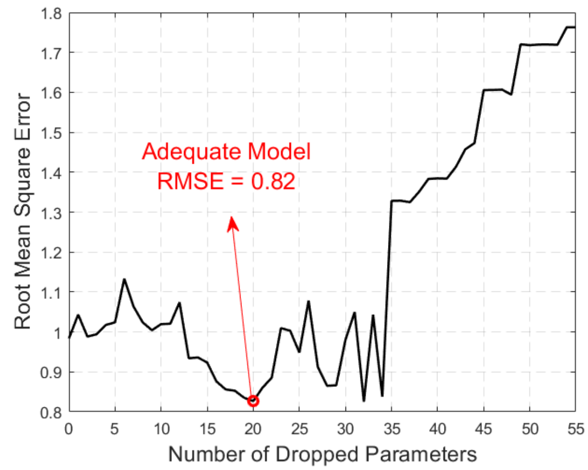

Figure 6. Variation of RMSE through model reduction in 70 knots forward flight

leads to jumps in the cost function, as can be seen in fig. 6. For the forward flight case, the adequate model is again selected where the RMSE is the lowest, which corresponds to the model structure with 20 parameters removed. With the selected model, the time domain error criteria $\mathrm{RMSE} \leq 1.0$ to 2.0 is satisfied. With the model reduction procedure, the derivatives X_v, X_q, X_r, X_{ped}, Y_u, Y_w, Y_q, Y_r, Y_{long}, Y_{coll}, Z_v, Z_p, Z_q, Z_{lat}, Z_{ped}, L_{ped}, M_u, M_v, M_{ped} and N_u are dropped from the model structure. The examination of the selected model in time and frequency domains showed that the inclusion of time delays is again necessary to reflect the higher order dynamics.

The key stability derivatives have been validated against Padfield's reference for similar helicopters (Ref. 24) to ensure that they align with rotorcraft dynamics: The angle of attack static stability derivative, M_w, is particularly important in forward flight due to the influence of the horizontal tail. The horizontal tail generates a restoring moment, resulting in a negative M_w. The dihedral effect, represented by L_v, remains negative as in hover, indicating a stabilizing roll response to sideslip. The weathercock stability derivative, N_v, is positive in forward flight, with the vertical tail contributing to the restoring yaw moment alongside the tail rotor. The heave stability derivative, Z_w, has a negative sign similar to hover. Overall, the identified parameters with the minimal system representation are found to be consistent with helicopter dynamics. Similar to the hover case, the parameters and their bounds can be seen in Appendix B.

The identification models with and without time delays are compared with the truth model for the cyclic tests in time domain. Figures 7 and 8 show the responses of the three models for 2311 type inputs. The lag of the truth model can be clearly seen in the off-axis response of the longitudinal cyclic maneuver. With the introduction of time delays, the improvement on the model fit is clearly observable. The improvement with the time de-

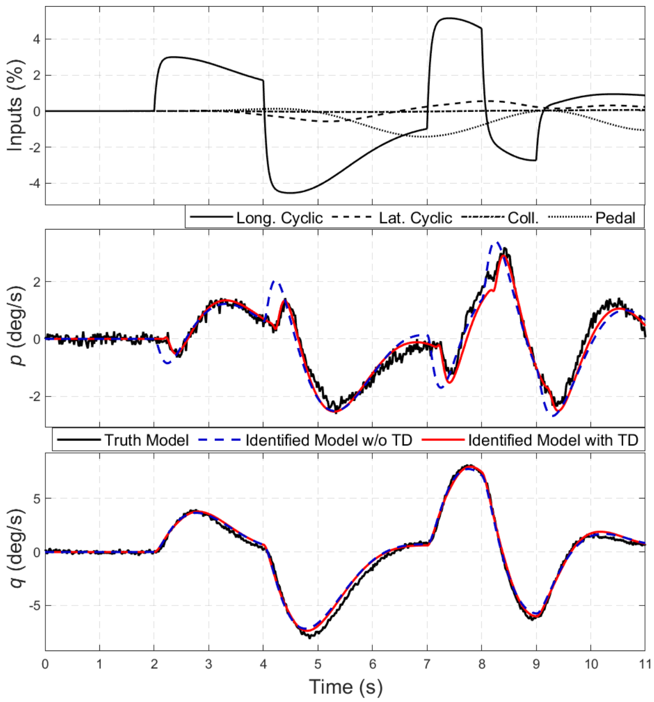

Figure 7. Time domain identification results - longitudinal cyclic 2311 input in positive direction in 70kts forward flight

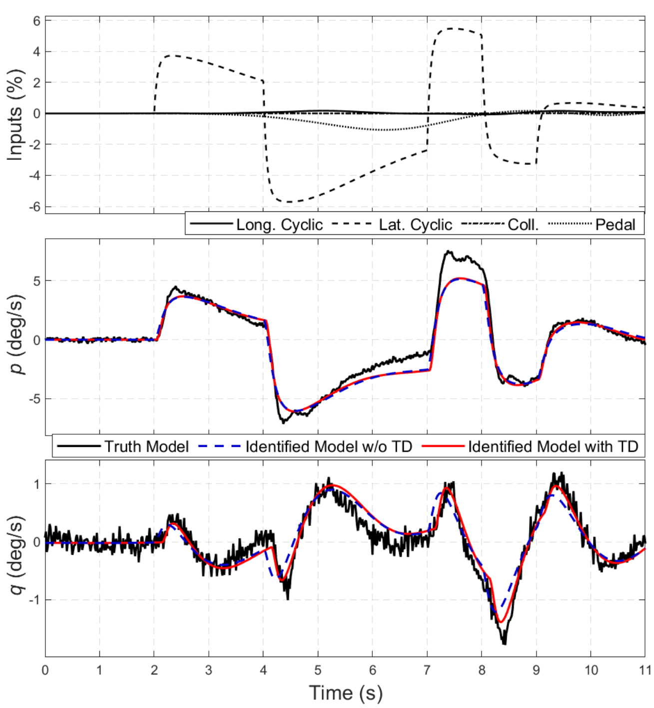

Figure 8. Time domain identification results - lateral cyclic 2311 input in positive direction in 70kts forward flight

lays are also seen in the frequency responses, as shown in figs. 9 and 10. While the magnitude and on-axis phase error characteristics fall within the MUAD bounds and AEE, the off-axis errors are diminished significantly with the employment of time delays. Therefore, the identified model fit is determined to be satisfactory in bot time and frequency domains.

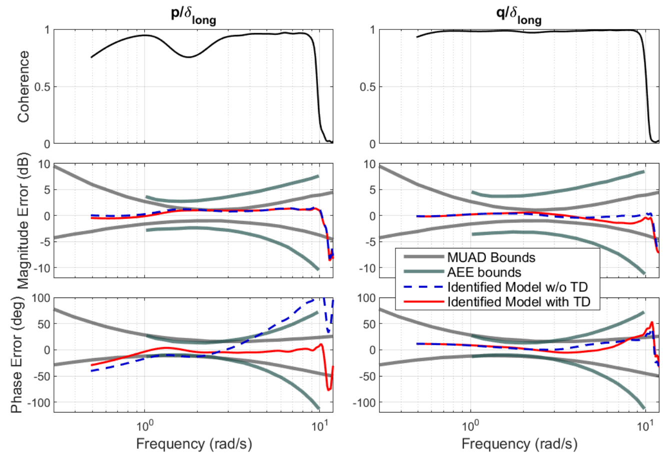

Figure 9. q/δ_{long} and p/δ_{long} pairs with error bounds - longitudinal cyclic frequency sweep maneuver in 70kts forward flight

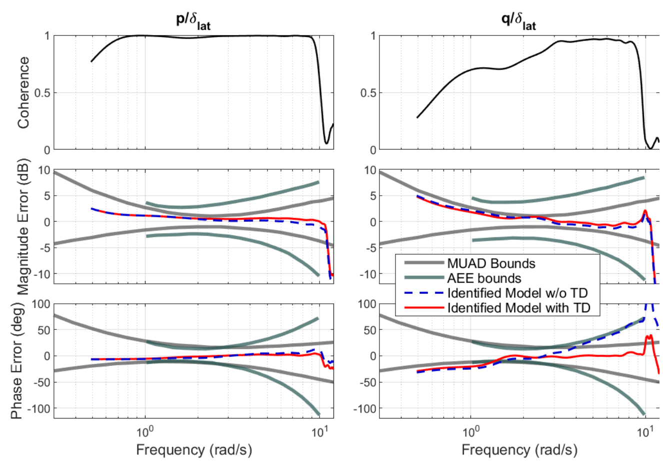

Figure 10. q/δ_{lat} and p/δ_{lat} pairs with error bounds - lateral cyclic frequency sweep maneuver in 70kts forward flight

CONCLUSIONS

This study presents a standalone time-domain identification of a full-scale helicopter dynamics, in two flight conditions, using the output error algorithm. The following conclusions can be drawn from the presented work:

1. By employing a systematic model reduction routine based on Cramer-Rao and insensitivity metrics, a

minimal model representation is achieved. This representation increases confidence in the model parameter estimations, as it drives the estimations towards their physical values. It is shown that the aerodynamic derivatives are consistent with helicopter dynamics.

2. Owing to the flexibility of the output error algorithm to handle systems of any level of complexity, time delays can be introduced into any model parameter. It is demonstrated that with the implementation of time delays into the key parameters, the higher order dynamics due to the rotor can be represented in both time and frequency domain responses.

3. The identified models are validated as sufficient, with the frequency response function errors falling within the bounds of both the MUAD and AEE criteria.

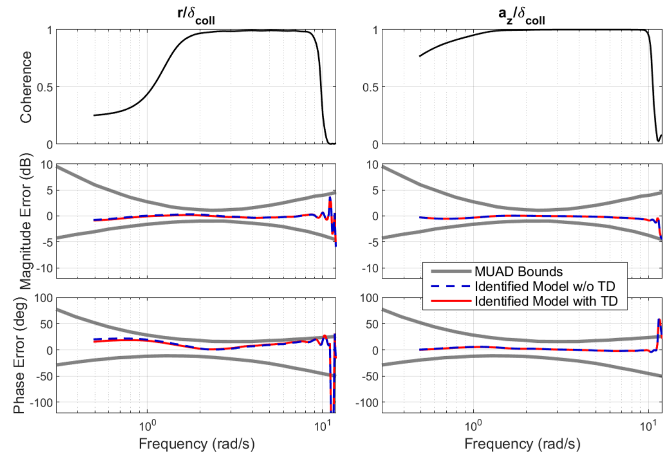

Figure 12. r/δ_{coll} **and** a_z/δ_{coll} **pairs with error bounds - collective frequency sweep maneuver in hover**

Author contact:
Ongun Hazar Aslandoğan
ongunhazar.aslandogan@tum.de
Gönenç Gürsoy gonencgursoy@gmail.com
İlkay Yavrucuk ilkay.yavrucuk@tum.de

APPENDIX A

Collective and Pedal Identification Results in Hover

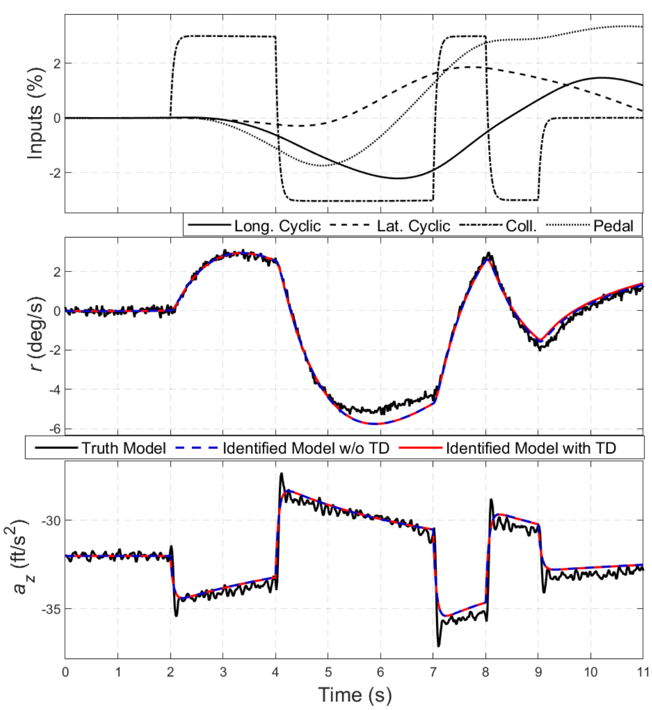

Figure 11. Time domain identification results - collective 2311 input in positive direction during hover

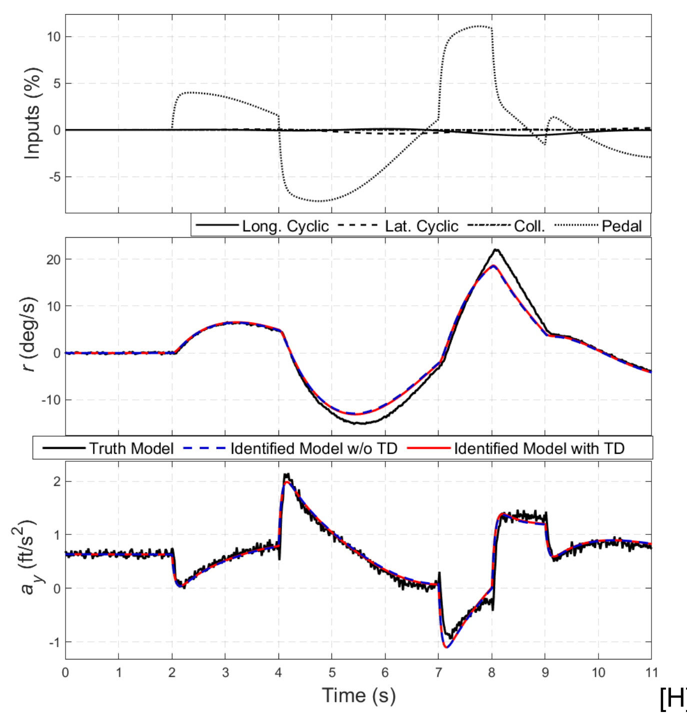

Figure 13. Time domain identification results - pedal 2311 input in positive direction during hover

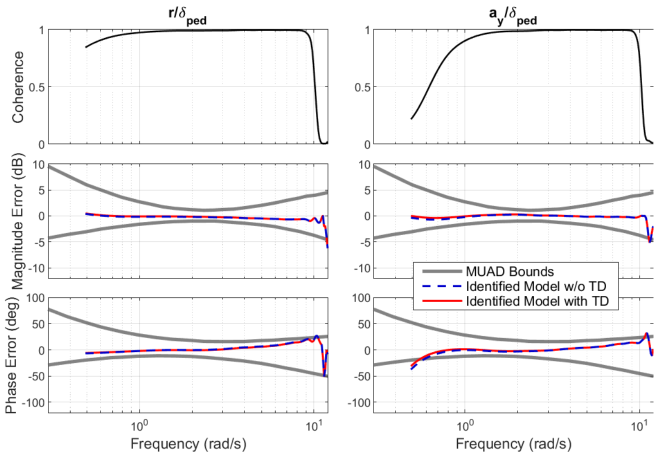

Figure 14. r/δ_{ped} **and** a_y/δ_{ped} **pairs with error bounds - pedal frequency sweep maneuver in hover**

Collective and Pedal Identification Results in Forward Flight

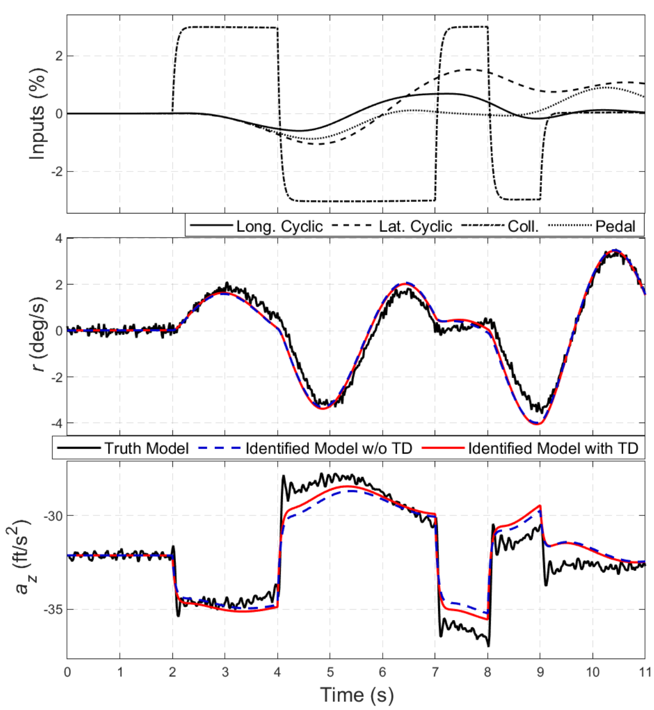

Figure 15. Time domain identification results - collective 2311 input in positive direction in 70kts forward flight

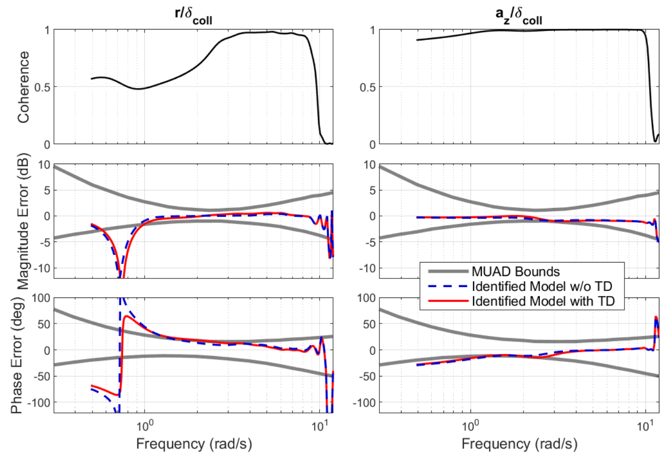

Figure 16. r/δ_{coll} **and** a_z/δ_{coll} **pairs with error bounds - collective frequency sweep maneuver in 70kts forward flight**

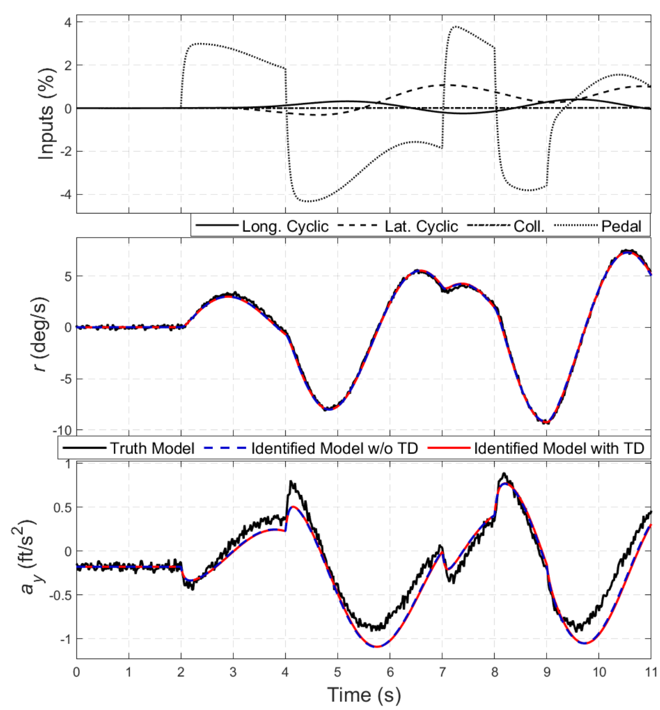

Figure 17. Time domain identification results - pedal 2311 input in positive direction in 70kts forward flight

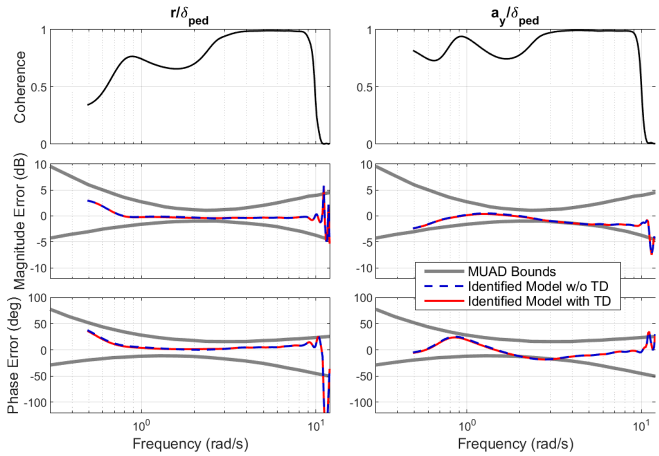

Figure 18. r/δ_{ped} **and** a_y/δ_{ped} **pairs with error bounds - pedal frequency sweep maneuver in 70kts forward flight**

REFERENCES

1. Kaufman, L. and Peress, K., "A review of methods for predicting helicopter longitudinal response," *Journal of the Aeronautical Sciences*, Vol. 23, No. 3, 1956, pp. 259–271.

2. Marchand, M. and Kh, F., "Frequency domain parameter estimation of aeronautical systems without and with time delay," *IFAC Proceedings Volumes*, Vol. 18, No. 5, 1985, pp. 669–674.

3. Tischler, M., Leung, J., and Dugan, D., "Frequency-domain identification of XV-15 tilt-rotor aircraft dynamics," *2nd Flight Testing Conference*, 1983, p. 2695.

4. Tischler, M. B., Fletcher, J. W., Diekmann, V. L., Williams, R. A., and Cason, R. W., "Demonstration of frequency-sweep testing technique using a Bell 214-ST helicopter," Tech. rep., National Aeronautics and Space Administration Moffett Field CA AMES …, 1987.

5. Seher-Weiss, S. and von Grünhagen, W., "Comparing explicit and implicit modeling of rotor flapping dynamics for the EC 135," *CEAS Aeronautical Journal*, Vol. 5, No. 3, 2014, pp. 319–332.

6. Seher-Weiss, S., "Comparing different approaches for modeling the vertical motion of the EC 135," *CEAS Aeronautical Journal*, Vol. 6, No. 3, 2015, pp. 395–406.

7. Seher-Weiß, S., "ACT/FHS system identification including rotor and engine dynamics," *Journal of the American Helicopter Society*, Vol. 64, No. 2, 2019, pp. 1–12.

8. Li, P. and Postlethwaite, I., "Subspace and bootstrap-based techniques for helicopter model identification," *Journal of the American Helicopter Society*, Vol. 56, No. 1, 2011, pp. 12002–12002.

9. Shim, D. H., Kim, H. J., and Sastry, S., "Control system design for rotorcraft-based unmanned aerial vehicles using time-domain system identification," *Proceedings of the 2000. IEEE International Conference on Control Applications. Conference Proceedings (Cat. No. 00CH37162)*, IEEE, 2000, pp. 808–813.

10. Khaligh, S. P., Fahimi, F., and Robert Koch, C., "A system identification strategy for nonlinear model of small-scale unmanned helicopters," *Journal of the American Helicopter Society*, Vol. 61, No. 4, 2016, pp. 1–13.

11. Grauer, J., Conroy, J., Hubbard Jr, J., Humbert, J., and Pines, D., "System identification of a miniature helicopter," *Journal of Aircraft*, Vol. 46, No. 4, 2009, pp. 1260–1269.

12. Berger, T., Tobias, E. L., Tischler, M. B., and Juhasz, O., "Advances and Modern Applications of Frequency-Domain Aircraft and Rotorcraft System Identification," *Journal of Aircraft*, Vol. 60, No. 5, 2023, pp. 1331–1353.

13. Jategaonkar, R., *Flight Vehicle System Identification: A Time-Domain Methodology, Second Edition*, 02 2015.

14. Aerotim Engineering, https://www.aerotim.com.tr, [Accessed February 2024].

15. Marquardt, D. W., "An algorithm for least-squares estimation of nonlinear parameters," *Journal of the society for Industrial and Applied Mathematics*, Vol. 11, No. 2, 1963, pp. 431–441.

16. Tischler, M. and Remple, R., *Aircraft And Rotorcraft System Identification: Engineering Methods With Flight-test Examples*, 08 2006.

17. Gursoy, G., Aslandogan, O. H., and Yavrucuk, I., "Linear Model Identification for Rotorcraft Using Adaptive Learning," *Proceedings of the 77th Annual Forum*, The Vertical Flight Society, Virtual, May 2021.

18. Maine, R. E. and Iliff, K. W., "The theory and practice of estimating the accuracy of dynamic flight-determined coefficients," Tech. rep., 1981.

19. Hoh, R. H., Mitchell, D. G., Ashkenas, I. L., Klein, R. H., and Heffley, R. K., "Proposed MIL Standard and Handbook-Flying Qualities of Air Vehicles. Volume 2. Proposed MIL Handbook," Tech. rep., Systems Technology Inc Hawthorne CA, 1982.

20. Mitchell, D., Hoh, R., He, C., and Strope, K., "Determination of maximum unnoticeable added dynamics," *AIAA Atmospheric Flight Mechanics Conference and Exhibit*, 2006, p. 6492.

21. Cicolani, L. S., McCoy, A. H., Sahai, R., Tyson, P. H., Tischler, M. B., Rosen, A., and Tucker, G. E., "Flight Test Identification and Simulation of a UH-60A Helicopter and Slung Load," *Journal of the American Helicopter Society*, Vol. 46, No. 2, 2001, pp. 140–160.

22. Myrand-Lapierre, V., Tischler, M. B., Pavel, M. D., Nadeau-Beaulieu, M., Stroosma, O., Gubbels, B., and White, M., "Bell 412 modeling and model fidelity assessment for level-d training simulators," *Vertical Flight Society's 76th Annual Forum and Technology Display*, 2020.

23. Tischler, M. B., Scepanovic, P., Gubbels, A., et al., "Bell 412 system identification and model fidelity assessment for hover and forward flight," *Journal of the American Helicopter Society*, Vol. 66, No. 1, 2021, pp. 1–13.

24. Padfield, G. D., *Helicopter flight dynamics: the theory and application of flying qualities and simulation modelling*, John Wiley & Sons, 2008.